Research on Distribution Transformer Layout Planning Model of Distribution Networks Considering the Impact of Distributed Generation and Electric Vehicles

Wenzhong Wang[1], Jinxing Zhong[1], Jinping Zhang[2] and Juan Zhang[2,*]

[1]*Dongguan Power Supply Bureau of Guangdong Power Grid Co., Ltd, Guangdong Province, China*
[2]*Tianjin Tianda Qiushi Electric Power High Technology Co., Ltd, Tianjin, China*
E-mail: 708959377@qq.com
[*]*Corresponding Author*

Received 29 November 2025; Accepted 25 January 2026

Abstract

Under the background of the "dual-carbon" strategy and the ongoing energy structure transition, the rapid penetration of distributed generation (DG) and electric vehicles (EVs) has introduced bidirectional uncertainties on both the supply and demand sides of distribution networks. To address the limitations of traditional transformer planning methods that fail to simultaneously capture the stochastic characteristics of DG and EVs, this paper proposes a multi-objective optimization model for transformer layout planning considering source-load uncertainties. The model characterizes the stochastic outputs of photovoltaic and wind power using Beta and Weibull distributions, respectively, and adopts a Monte Carlo simulation framework to represent the spatiotemporal distribution patterns of EV charging loads, thereby achieving

Strategic Planning for Energy and the Environment, Vol. 45_2, 461–486.
doi: 10.13052/spee1048-5236.4527

coordinated modeling of source-load randomness. On this basis, a probabilistic optimization framework is established to minimize the total life-cycle cost-including transformer investment, network losses, and outage losses-subject to voltage, current, and capacity constraints. Simulation results on the enhanced IEEE 33-bus network verify that the proposed method can effectively improve voltage regulation, cut line losses and operating costs, and sustain system stability under substantial DG and EV penetration. The research provides a systematic modeling approach and optimization reference for transformer planning in distribution networks with high renewable energy and EV integration.

Keywords: Distributed generation, electric vehicles, transformer layout, probabilistic power flow.

1 Introduction

Against the backdrop of the continuous advancement of the "dual-carbon" goals and the deep adjustment of the global energy structure [1–3], DG and EVs have become the core driving forces and key influencing factors in the upgrading of distribution networks. On the one hand, DG technologies represented by photovoltaic (PV) and wind turbine (WT) align closely with the requirements of energy transition due to their clean and low-carbon characteristics. As of September 2023, China's cumulative installed capacity of distributed PV has exceeded 105 GW, making it a crucial component of the clean energy system in distribution networks. On the other hand, as the main carrier of transportation electrification, the number of EVs has been increasing annually, and their role is gradually transforming into a major load within distribution networks. The large-scale, coordinated integration of DG and EVs has disrupted the traditional radial structure of single-source distribution networks, accelerating their evolution into complex systems with multiple sources and diverse loads. However, this transformation also brings significant challenges associated with increasing uncertainties on both the supply and demand sides.

From the supply perspective, DG output is highly dependent on meteorological conditions: PV generation exhibits intermittency due to diurnal variations in solar irradiance and cloud coverage, while wind power output fluctuates with stochastic wind speed changes, leading to instability. From the demand perspective, EV charging load exhibits strong temporal and spatial randomness, with residential charging typically concentrated during the

evening peak hours of 18:00–22:00. The superposition of these uncertainties on both sides tends to exacerbate voltage fluctuations, increase line losses, and reduce transformer capacity margins [4–8], thereby posing serious threats to the stability and reliability of power supply in distribution networks.

Extensive research has explored the impacts of DG and EVs on distribution network operation from multiple perspectives. In DG modeling, [9] employed the Beta distribution to characterize PV output and the Weibull distribution to describe wind speed variability. Reference [10] proposed a hybrid optimization approach combining tabu search and the Chu-Beasley genetic algorithm to simultaneously optimize the siting and sizing of dispatchable/stochastic DG and fixed/switchable capacitor banks. Reference [11] developed a two-level cooperative model predictive control strategy for distributed PV systems, where the upper level ensures coordinated operation of all PV units at a common available power ratio, and the lower level applies dynamic matrix control to track reference signals. Reference [12] presented a multi-period optimization strategy based on the GRASP-TS metaheuristic algorithm, which jointly evaluates the maximum hosting capacity of renewable DG and EVs under operational constraints by coordinating EV charging and DG curtailment. To address unbalanced voltage and undervoltage issues caused by high DG and EV penetration in low-voltage networks, Reference [13] proposed a multi-objective optimization method based on differential evolution. Reference [14] introduced an autonomous EV charging coordination method using fitted Q-iteration reinforcement learning to enhance system flexibility and PV utilization. Reference [15] proposed a consumer-oriented multi-objective optimization framework integrating distribution and transportation networks, where an improved weighted teaching–learning-based particle swarm optimization algorithm was used to jointly optimize the siting and sizing of EV charging stations and DGs in three stages. Reference [16] focuses on the impact of EV charging on the power quality of distribution networks. Through case studies, hardware-in-the-loop simulation models, and field measurement data, it integrates key parameters such as short-circuit power, power factor, and harmonic distortion, and proposes the Electric Vehicle Charging Grid Impact Index. This index enables predictive assessment of the potential impacts of charging facilities on the power grid, thereby providing a supportive tool for grid management and the expansion of charging infrastructure. Reference [17] focuses on the modeling and analysis of integrating renewable energy and EVs into microgrids. It investigates the effects of EV charging and discharging on microgrid power quality, harmonics, and

voltage, and further discusses V2G technology, charging infrastructure, and various control strategies. Reference [18] analyzes real-world data on EV users' driving and charging behaviors and applies the Bootstrap method to determine that a time step shorter than 10 minutes can ensure a confidence level of over 95%. The study finds that only about 40% of EVs are plugged in simultaneously, and approximately half of them are suitable for V2G operation. Based on these findings, the reference proposes corresponding charging management recommendations. Reference [19], from the perspective of distribution system operators, proposes a multi-period optimization strategy based on the GRASP-TS metaheuristic algorithm. By coordinating operational resources such as EV aggregator charging and optimizing DG curtailment, the method simultaneously evaluates the maximum hosting capacity of renewable DG and EVs in distribution networks. The algorithm features fast convergence and strong scalability. Reference [20] proposes a framework that integrates the Whale Optimization Algorithm, CNN-BiLSTM, Copula Model, and Nonparametric Kernel Density Estimation for multi-time scale short-term wind farm power forecasting and uncertainty analysis.

In summary, although existing studies have made considerable progress in DG and EV modeling, load forecasting, and optimal scheduling, several limitations remain in terms of systematic modeling and optimization for transformer planning: Most studies treat DG and EV impacts separately, lacking a unified framework for coordinated modeling and quantification of source-load uncertainties; Traditional deterministic planning approaches fail to reflect the stochastic characteristics of DG generation and EV charging behaviors, leading to transformer capacity configurations deviating from actual operational demands; Existing cost models primarily focus on investment or energy losses, without fully considering the dynamic variation of life-cycle costs or their coupling relationship with voltage stability.

To tackle the aforementioned issues, this study develops a multi-objective optimization framework for transformer allocation in distribution networks, incorporating the coupled uncertainties of DG and EV integration. The primary innovations of this work can be outlined as follows:

- Source-load uncertainty modeling: The stochastic characteristics of PV and wind generation are modeled using the Beta and Weibull distributions, respectively, while the spatiotemporal distribution of EV charging loads is simulated using the Monte Carlo method to achieve unified modeling of source–load randomness;

- Optimization framework: A multi-objective optimization model is constructed under probabilistic power flow constraints, minimizing the life-cycle costs of transformer investment, network losses, and outage losses to balance economic efficiency and operational reliability;
- Solution methodology: A hybrid solution strategy combining uncertainty scenario generation and robust optimization is proposed to enhance the stability and adaptability of planning decisions under high DG and EV penetration.

The proposed research provides a generalized modeling framework and decision-making reference for transformer planning in distribution networks with high DG and EV integration, offering both theoretical significance and practical value for achieving low-carbon, intelligent, and resilient power distribution systems.

2 Modeling of Source-Load Characteristics in Distribution Networks

2.1 Distributed Generation Characteristic Model

In this study, two typical types of DG-PV and WT are selected as research objects. Since their output power is significantly affected by meteorological conditions and exhibits strong random fluctuations, probabilistic and statistical methods are required to characterize their inherent uncertainties.

2.1.1 PV output model

The output of a photovoltaic (PV) system is primarily influenced by variations in solar irradiance. Solar radiation exhibits both periodic and instantaneous fluctuations over time, resulting in significant randomness in PV power output. To represent this characteristic, the solar irradiance can be modeled as a random variable following a Beta distribution [21], and its probability density function $f(\xi)$ is used to describe the statistical distribution of irradiance:

$$f(\xi) = \frac{\Gamma(\alpha+\beta)}{\Gamma(\alpha)\Gamma(\beta)} \left(\frac{\xi}{\xi_{\max}}\right)^{\alpha-1} \left(1-\frac{\xi}{\xi_{\max}}\right)^{\beta-1} \tag{1}$$

where $\Gamma(\cdot)$ stands for the Gamma function; α and β are the Beta distribution parameters derived from the mean and standard deviation of solar irradiance; ξ and ξ_{max} correspond to the observed and maximum irradiance values.

Consequently, the probability density function of photovoltaic output power, denoted as $f(P_{PV})$, can be formulated as:

$$f(P_{PV}) = \frac{\Gamma(\alpha+\beta)}{\Gamma(\alpha)\Gamma(\beta)} \left(\frac{P_{PV}}{P_{PV,\max}}\right)^{\alpha-1} \left(1 - \frac{P_{PV}}{P_{PV,\max}}\right)^{\beta-1} \tag{2}$$

$$\begin{cases} P_{PV} = \xi A \eta_e \\ \alpha = \mu_{PV} \left[\dfrac{\mu_{PV}(1-\mu_{PV})}{\sigma_{PV}^2} - 1\right] \\ \beta = (1-\sigma_{PV}) \left[\dfrac{\sigma_{PV}(1-\sigma_{PV})}{\sigma_{PV}^2} - 1\right] \end{cases} \tag{3}$$

Where μ_{pv} and σ_{pv} denote the mean and variance of solar irradiance, respectively; A represents the effective irradiance receiving area; η_e is the energy conversion efficiency between solar energy and electrical energy; P_{PV} and $P_{\mathrm{PV,max}}$ denote the actual and maximum active power outputs of the PV system, respectively.

Once the probability distribution of solar irradiance is determined, the probabilistic model of PV output can be obtained by exploiting the linear relationship between photovoltaic power generation and solar irradiance, expressed as:

$$P_{pv,t,i} = r_{t,i} A_{t,i} \eta_i \tag{4}$$

Where $P_{t,i}$ denotes the active power output of the *i*-th PV station at time t, $A_{t,i}$ denotes the effective area of the corresponding PV module, η_i represents the energy conversion efficiency of the *i*-th photovoltaic station.

2.1.2 WT output model

The time-varying characteristics of wind speed are the primary cause of the stochastic fluctuations in wind power output and serve as a crucial basis for performance analysis and power calculation of wind power systems. Since the distribution of wind speed is significantly influenced by geographical and meteorological conditions, it is difficult to describe it deterministically and it typically exhibits an asymmetric distribution pattern. To accurately capture its statistical behavior, appropriate probabilistic distribution models are commonly employed for fitting. Among them, the Weibull distribution is widely used for wind speed characterization due to its concise mathematical form, flexible parameters, and strong ability to match measured wind speed data. The relationship between wind turbine output

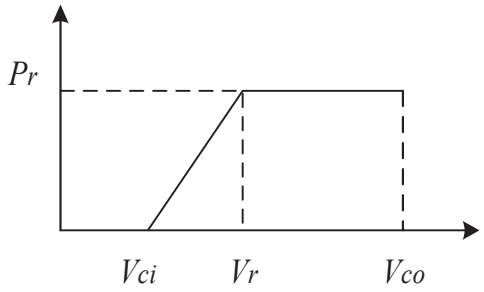

Figure 1 Variation of wind induction generator power output with wind speed.

power and wind speed exhibits a piecewise characteristic, as illustrated in Figure 1.

Where P_r is the rated power, V_{ci} is the cut-in wind speed, V_r is the rated wind speed, and V_{co} is the cut-out wind speed. The slope and intercept of the linear segment are denoted by k_1 and k_2, respectively.

The probability density function of the two-parameter Weibull distribution can be written as:

$$f(v) = \frac{k}{c}\left(\frac{v}{c}\right)^{k-1} e^{-\left(\frac{v}{c}\right)^k} \tag{5}$$

Where *k* and *c* are the shape and scale parameters of the Weibull distribution, respectively. These parameters can be estimated using the sample mean and standard deviation of wind speed. Given the sample mean μ and standard deviation σ, the following relationships hold:

$$k = \left(\frac{\sigma}{\mu}\right)^{-1.086} \tag{6}$$

$$c = \frac{\mu}{\Gamma(1+1/k)} \tag{7}$$

The probability density function of the active power output of wind generation can be expressed as:

$$f(P_{WT}) = \frac{k}{k_1 c}\left(\frac{P_{WT}-k_2}{k_1 c}\right)^{k-1} \exp\left[-\left(\frac{P_{WT}-k_2}{k_1 c}\right)^k\right] \tag{8}$$

Then, if the cut-in and cut-out wind speeds of the *i*-th wind turbine are set as $\underline{V_i}$ and $\overline{V_i}$ respectively, the time-series output power model of the wind

turbine can be expressed as:

$$P_{wt,t,i} = \begin{cases} 0 & v_{t,i} \le \underline{V_i} \\ \dfrac{P_{N,i}}{V_N - \underline{V_i}} v_{t,i} - \dfrac{P_{N,i}}{V_N - \underline{V_i}} \underline{V_i} & \underline{V_i} \le v_{t,i} \le V_N \\ P_{N,i} & V_N \le v_{t,i} \le \overline{V_i} \\ 0 & v_{t,i} \ge \overline{V_i} \end{cases} \tag{9}$$

The parameters of the Beta and Weibull distributions are estimated from the sample mean and standard deviation of historical solar irradiance and wind speed data, respectively. Variations in these parameters affect the dispersion and tail behavior of DG output scenarios generated by the Monte Carlo process, which in turn influence probabilistic power flow results and transformer capacity configuration by altering the frequency of extreme operating conditions.

2.2 EV Charging Load Model

The large-scale penetration of EVs into the power grid tends to elevate system load peaks, exhibiting an effect comparable to that of DG integration, and consequently poses challenges to grid security and operational stability. In this study, the daily driving distance of residential EVs is assumed to follow a lognormal distribution [22], expressed as:

$$f_s(x) = \frac{1}{x} \frac{1}{\sigma_s \sqrt{2\pi}} \exp\left(-\frac{(\ln x - \mu_s)^2}{2\sigma_s^2} \right) \tag{10}$$

Where the mean value is set as $\mu_s = 3$, and the variance as $\sigma_s = 0.8$.

The starting charging time is assumed to follow a normal distribution, that is:

$$f_t(x) = \begin{cases} \dfrac{1}{\sigma_s \sqrt{2\pi}} \exp\left(-\dfrac{(x - \mu_s)^2}{2\sigma_s^2} \right) & \mu_s - 12 < x < 24 \\ \dfrac{1}{\sigma_s \sqrt{2\pi}} \exp\left(-\dfrac{(x + 24 - \mu_s)^2}{2\sigma_s^2} \right) & 0 < x < \mu_s - 12 \end{cases} \tag{11}$$

The total charging load of EVs can be expressed as:

$$P_{EV} = \sum_{i=1}^{N_{EV}} P_{EV,i} \bullet \delta_i(t) \tag{12}$$

Here, N_{EV} denotes the number of EVs in the distribution area, and $\delta(t)$ is a binary variable, where $\delta(t) = 1$ indicates that the *i*-th is charging at time t.

3 Probabilistic Power Flow Modeling for Distribution Networks

Using the time-series generation and load models for DGs and EVs introduced above, this chapter establishes a probabilistic power flow framework for distribution networks and proposes the corresponding computational methodology. The proposed method is designed to effectively address the uncertainties arising from DG integration, thereby improving voltage stability and mitigating power losses within the distribution system.

3.1 Objective Function

Taking into account the operational costs and voltage regulation requirements of Active Distribution Networks (ADNs), this study formulates an objective function that minimizes a linearly weighted sum of system loss costs, switching operation costs, and overall voltage deviation:

$$f_{\min} = W_T f_{\text{loss}} + W_v f_v \tag{13}$$

Where W_T and W_v are coefficients determined by the Analytic Hierarchy Process [23]; f_{loss} refers to the system loss cost, and $\underline{f}_v$ indicates the magnitude of voltage deviation within the system:

$$f_{\text{loss}} = C_{\text{loss}} \left(\sum_{t=1}^{N_T} \sum_{ij \in \Omega} r_{ij} I_{t,ij}^2 \Delta t + \sum_{t=1}^{N_T} \sum_{i=1}^{N_N} P_{t.i}^{\text{DT,loss}} \Delta t \right) \tag{14}$$

Where C_{loss} is the cost coefficient of system losses; N_T denotes the calculation period; brepresents the set of branches excluding the newly added DT; r_{ij} is the resistance of branch $i - j$; $I_{t,ij}$ is the current of branch $i - j$ at time t, which must satisfy the line current-carrying capacity constraint as shown in Equation; Δt is the unit time interval; N_N denotes the total number of system nodes; and $P_{t.i}^{\text{DT,loss}}$ represents the power flowing through the newly added DT at time t.

To ensure that the voltage remains within the desired range, fv is defined using a voltage interval control strategy, expressed as follows:

$$f_v = \sum_{t=1}^{N_T} \sum_{i=1}^{N_N} |U_{t,i}^2 - U^2| \tag{15}$$

Where $U_{t,i}$ and U represent the voltage at node i and the desired voltage range at time t, respectively. They satisfy the following conditions:

3.2 Constraints

3.2.1 System constraints

The system constraints mainly include the operating constraints of the distribution network and the operational constraints of power flow control devices:

$$\sum_{ij\in\Omega_b}(P_{t,ij}-r_{ij}I_{t,ij}^2)+P_{t,j}+\sum_{ij\in\Omega_0}P_{t,ij}^{\mathrm{DT}}=\sum_{ik\in\Omega_b}P_{t,jk}+\sum_{ij\in\Omega_0}P_{t,jk}^{\mathrm{DT}} \tag{16}$$

$$\sum_{ij\in\Omega_b}(Q_{t,ij}-x_{ij}I_{t,ij}^2)+Q_{t,j}+\sum_{ij\in\Omega_0}Q_{t,ij}^{\mathrm{DT}}=\sum_{ik\in\Omega_b}Q_{t,jk}+\sum_{ij\in\Omega_0}Q_{t,jk}^{\mathrm{DT}} \tag{17}$$

$$U_{t,i}^2-U_{t,j}^2-2(r_{ij}P_{t,ij}+x_{ij}Q_{t,ij})+(r_{ij}^2+x_{ij}^2)I_{t,ij}^2=0 \tag{18}$$

$$U_{t,ij}^2I_{t,ij}^2=P_{t,ij}^2+Q_{t,ij}^2 \tag{19}$$

Where Ω_b denotes the set of branches excluding the newly added DT; $P_{t,ij}$ and $Q_{t,ij}$ represent the active and reactive power of branch $i-j$ at time t; x_{ij} denotes the reactance of branch $i-j$; $P_{t,j}$ and $Q_{t,j}$ represent the total active and reactive power injections at node j at time t; $P_{t,ij}^{\mathrm{DT}}$ and $Q_{t,ij}^{\mathrm{DT}}$ denote the active and reactive power of the newly added DT on branch $i-j$ at time t; $P_{t,jk}$ and $Q_{t,jk}$ represent the active and reactive power of branch $j-k$ at time t; $P_{t,jk}^{\mathrm{HDT}}$ and $Q_{t,jk}^{\mathrm{HDT}}$ denote the active and reactive power of the newly added DT on branch $j-k$ at time t; $P_{t,i}$ and $Q_{t,i}$ represent the total active and reactive power injections at node i at time t; $P_{t,i}$ and $Q_{t,i}$ represent the total active and reactive power at node i at time t.

The additional active and reactive power variables associated with newly installed distribution transformers represent the power transferred through these transformers at each time step. By acting as power transfer interfaces between upstream and downstream network segments, these variables enable the model to capture the role of transformer placement and sizing in voltage regulation, power flow allocation, and loss redistribution under stochastic operating conditions.

3.3 DG Operating Constraints

$$P_{t,i}^{\mathrm{DGs}} = P_{t,i}^{\mathrm{DGs},re} \tag{20}$$

$$Q_{t,i}^{\mathrm{DGs}} = P_{t,i}^{\mathrm{DGs}} \tan\theta_i^{\mathrm{DGs}} \tag{21}$$

$$\sqrt{(P_{t,i}^{\mathrm{DGs}})^2 + (Q_{t,i}^{\mathrm{DGs}})^2} \leq S_i^{\mathrm{DGs}} \tag{22}$$

Where $P_{t,i}^{\mathrm{DGs},re}$ 为 represents the predicted active power at node i at time t; θ_i^{DGs} denotes the power factor angle of the DGs at node i; S_i^{DGs} represents the installed capacity of the DGs at node i.

3.3.1 EV charging station power constraints

$$\begin{cases} P_{EV,\min} \leq P_{EV} \leq P_{EV,\max} \\ Q_{EV,\min} \leq Q_{EV} \leq Q_{EV,\min} \\ P_{EV}^2 + Q_{EV}^2 \leq S_{EV}^2 \end{cases} \tag{23}$$

Where P_{EV} and Q_{EV} denote the active and reactive power of the EV charging station, respectively; S_{EV} represents the rated capacity of the charging station.

4 Case Study

This study adopts an enhanced IEEE 33-bus distribution system as the test platform to validate the proposed probabilistic power flow approach for DT layout planning under high-DG-penetration conditions. Building on the original IEEE 33-bus model, structural and parametric modifications are introduced to incorporate DG and EV integration scenarios. The capacities, categories, and connection locations of various distributed generators and loads are explicitly configured to more accurately represent the operational characteristics of distribution networks with high penetration levels.

Using this refined model, power flow regulation simulations are performed in conjunction with DT layout planning. To account for source–load uncertainties, 100 stochastic input scenarios are generated using the Monte Carlo method as a compromise between computational efficiency and statistical representativeness. The stability of the simulation results is evaluated by examining key probabilistic indicators, including node voltage

probability distributions and the frequency distribution of the objective function. Comparative analyses of voltage profiles, branch current levels, network losses, and equipment switching frequencies under different control strategies show consistent statistical characteristics across scenarios, indicating that the selected number of scenarios is sufficient to ensure result robustness. Overall, the results demonstrate that the proposed optimization and planning framework substantially enhances voltage regulation capability and system robustness, while effectively reducing energy losses and switching actions in coordinated DG–EV high-penetration environments.

4.1 The Case Parameters

The topology of the improved IEEE 33-bus distribution system is shown in Figure 2, with the system's rated voltage $U_N = 12.66$ kV. In this study, the original network has been specifically adjusted to better reflect the actual operating characteristics under high-penetration scenarios of DG and EVs. The connection locations of DG units and EV charging loads are selected based on typical distribution network planning principles, including feeder length, load density, and practical suitability for renewable and transportation electrification integration. Specifically, DG units are installed at electrically weak or downstream buses to enhance local voltage support, while EV charging loads are distributed according to residential load concentration and travel electrification characteristics, improving the engineering representativeness and reproducibility of the case study.

The load at each bus primarily consists of EV charging demand, supplemented by basic residential and public service loads, thus forming a distribution pattern dominated by transportation electrification. By incorporating the EV charging power curve and its temporal distribution characteristics into

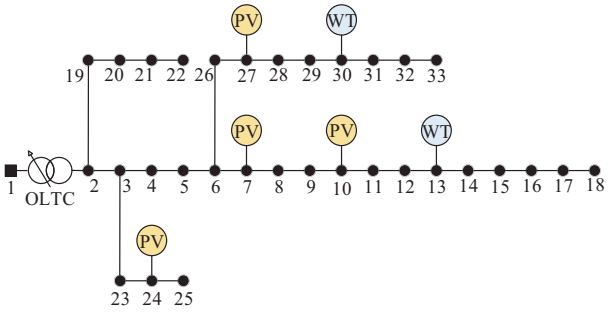

Figure 2 Improved IEEE 33-bus distribution system.

Table 1 Parameters of DGs

	Wind Turbine		Photovoltaic			
Access node	13	30	7	10	24	27
DG output rating (kVA)	800	1200	800	1200	800	1200

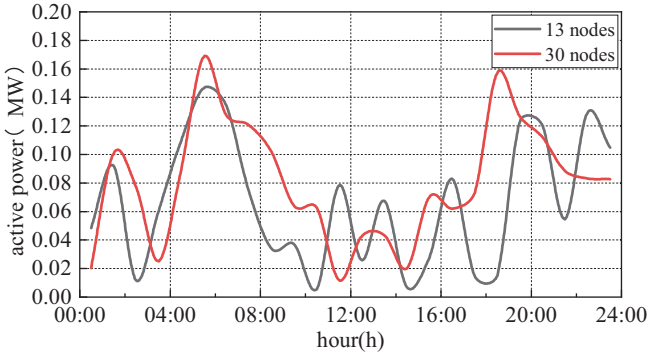

Figure 3 Output power of the wind turbine generator.

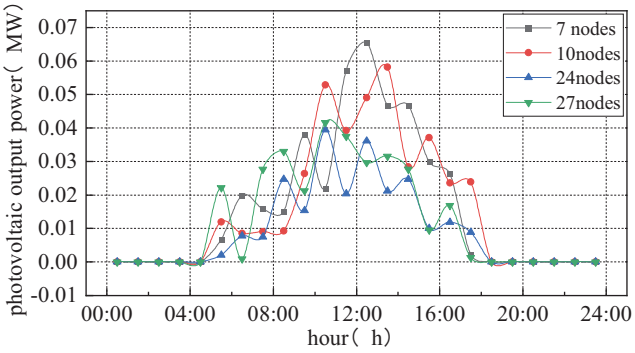

Figure 4 Output power of the PV station.

the power flow calculation process, the dynamic impact of charging behavior on bus voltage distribution and line power flow can be more accurately represented.

As illustrated in Figure 2, the case study system integrates wind turbine generators at buses 13 and 30, while distributed PV units are installed at buses 7, 10, 24, and 27. The operational parameters and output characteristics of the wind turbine at bus 13 and the PV installation at bus 7 are provided in Table 1, Figures 3, and 4, respectively.

4.2 Analysis of Effect

To verify the voltage security capability of the proposed distribution transformer layout planning model under high-penetration DG and EV integration conditions, this study generates 100 sets of source-load random scenarios using the Monte Carlo method after the planning optimization. Probabilistic power flow calculations are then performed, and the voltage probability distribution across all buses and time periods is statistically analyzed, as shown in Figure 5.

In the statistical results after planning optimization, the voltage probability density notably converges within the 0.96–1.00 pu range, while the probability in the low-voltage tail region is significantly reduced. This indicates that the overall network voltage distribution has shifted from a "wide-dispersion" pattern to a "concentrated" one, with both the fluctuation amplitude and the tail risk of occasional undervoltage substantially mitigated. From the perspective of the relationship between distribution characteristics and operational risk, this transformation can be interpreted as follows:

- Reduced dispersion implies that under the same level of source-load uncertainty, the sensitivity of node voltages to random disturbances decreases.
- Increased kurtosis and shortened left tail suggest that undervoltage events in extreme scenarios have been effectively "truncated."
- Improved quantile alignment reflects enhanced consistency of system performance across "worst-case–typical–best-case" conditions after planning.

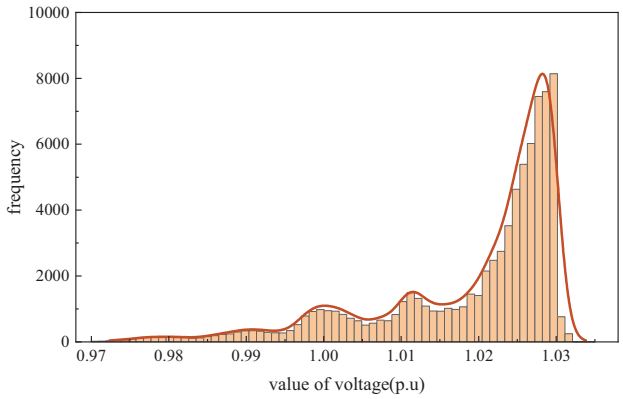

Figure 5 Voltage frequency distribution of all buses over the entire time horizon.

Considering the physical mechanism of source-load randomness, it can be observed that during the evening peak period – when EVs charge intensively and DG outputs fluctuate transiently – nodes at the network extremities and weakly supported regions are more prone to voltage drops before optimization. The proposed planning scheme, through optimized transformer sizing and placement, as well as coordinated reactive power and power flow path management, significantly enhances local voltage support and network stiffness. As a result, previously dispersed low-voltage samples are effectively "pulled back" toward the main peak region. It is worth noting that a very small probability of low-voltage tail events still remains after planning, which is attributable to unavoidable overlaps of extreme scenarios. However, both their occurrence probability and impact range have been substantially compressed, representing a controlled tail risk.

In summary, the threefold characteristics of main peak elevation, variance convergence, and tail shortening in the voltage frequency distribution statistically validate the proposed planning model's adaptability to DG/EV uncertainty and its systematic enhancement of voltage security margin. This provides a solid foundation for subsequent reliability assessments and operation–maintenance strategy coupling under probabilistic or chance-constrained frameworks.

To further characterize the post-planning voltage evolution of the system from a dual-scale perspective of nodes and time, this study selects Node 7 to illustrate its voltage contour distribution. First, Node 7 is chosen because it is located deep within the feeder and is adjacent to typical DG/EV access areas, thus exhibiting representative marginal node characteristics. Second, compared with central backbone nodes, this node's voltage is more sensitive to time-varying source-load disturbances, making it ideal for highlighting the planning scheme's voltage support effectiveness for weak nodes. Therefore, analyzing this node provides insights into potential voltage security bottlenecks. Third, instead of conventional line plots, the contour map format is adopted because it can simultaneously depict the relationships among time variation, voltage level, and probability density in a two-dimensional visualization. This enables a more intuitive representation of the continuous temporal evolution of voltage. Hence, employing a voltage contour map offers clear advantages in terms of time–amplitude joint visualization.

From the contour distribution, it can be observed that after planning optimization, the voltage at node 7 exhibits a continuously stable profile throughout the day. The voltage contour bands remain clearly continuous around the 0.97–1.00 pu range, with no longer any "high–low discontinuities"

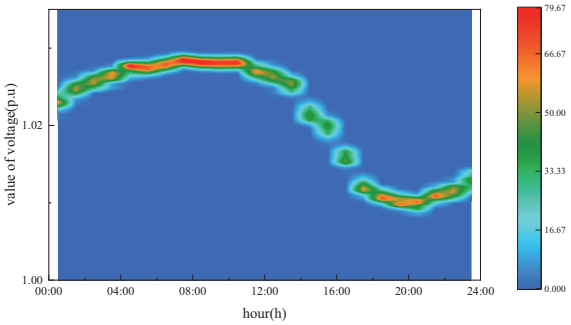

Figure 6 Voltage contour distribution at node 7.

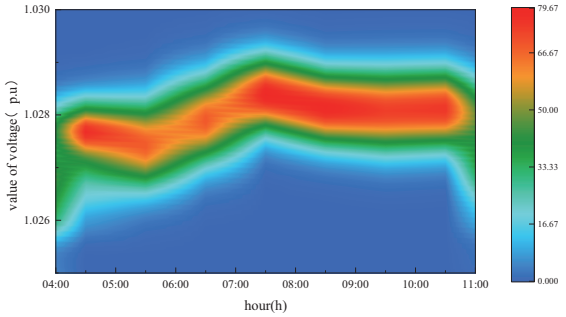

Figure 7 Local voltage profile from 4:00 to 11:00.

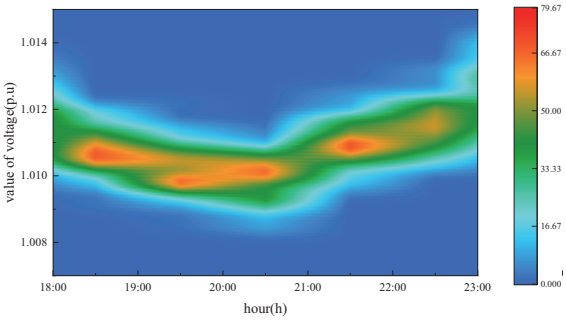

Figure 8 Local voltage profile from 18:00 to 11:00.

that existed before optimization. This indicates that the planning process not only improved the average voltage level but also effectively reduced temporal voltage nonuniformity. In addition, the voltage shows a slight rise during early-morning low-load periods and a mild drop during evening peak loads, yet it remains within the qualified range overall. This demonstrates that the

system, after optimization, can maintain a stable voltage support capability even under alternating "low-generation–high-load" conditions.

Furthermore, to enhance the interpretability of the temporal distribution characteristics, two typical time windows 4:00–11:00 and 18:00–21:00 are selected for localized magnification. The former represents the early morning to forenoon period, during which DG output gradually increases while EV load remains relatively low, characterizing a transition from "low-source to high-source" conditions. The latter corresponds to the evening peak when residents typically charge their EVs, representing a "high-load with insufficient DG support" scenario that is most unfavorable for voltage stability.

The localized contour maps provide a clearer depiction of the detailed "continuous voltage evolution over time." During the 4:00–11:00 window, as PV output gradually rises, the nodal voltage exhibits a smooth upward trend without noticeable jumps, indicating that the post-planning system maintains strong voltage buffering capability. In contrast, during the 18:00–21:00 high-load period, although the voltage experiences a slight decline, it remains within the desired range and the contour density shows no significant distortion. This demonstrates that the proposed planning effectively mitigates the voltage impact of concentrated EV charging on weak nodes.

In summary, the verification from three aspects-rationality of node selection, temporal continuity, and sensitivity under local extreme conditions-demonstrates that the post-planning distribution transformer layout significantly enhances the temporal voltage stability of weak boundary nodes. The voltage evolution transitions from a state of "frequent fluctuation" to one of "continuous smoothness," fully reflecting the proposed planning scheme's adaptability to source–load uncertainty and its effectiveness in ensuring voltage security.

To evaluate the economic efficiency and robustness of the proposed planning scheme under source–load uncertainty, this study performs batch calculations of the objective function across 100 Monte Carlo scenarios after optimization and plots the frequency distribution of the resulting objective values. The purposes of constructing this figure are threefold:

- Representation of stochastic cost variation: Because the objective function incorporates a linearly weighted sum of line loss cost, switching operation cost, and voltage deviation penalties, the resulting optimal operating cost is not deterministic. Instead, it behaves as a random variable influenced by the variability of DG and EV outputs. The frequency distribution effectively depicts the range of cost fluctuations across different stochastic scenarios.

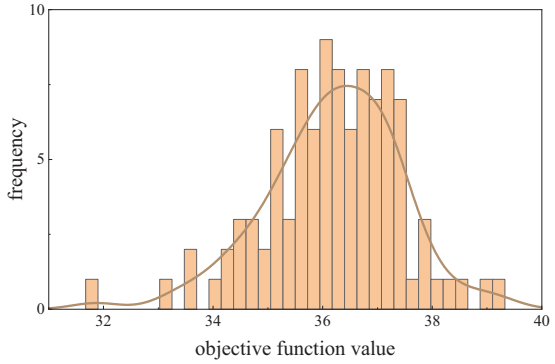

Figure 9 Histogram of objective function value frequency distribution.

- Capturing statistical characteristics: From the perspective of frequency, statistical dimensions such as mean, variance, skewness, and tail behavior can comprehensively describe how extreme scenarios affect economic performance, thereby overcoming the limitations of using a single expected value.
- Comparative analysis: By comparing the distribution shape before and after planning, one can visually assess the degree of improvement in cost concentration and tail risk mitigation, thus verifying the overall effectiveness of the proposed model in achieving the dual objectives of economy and security.

From the frequency distribution results of the objective function, it can be observed that after the planning optimization, the objective values exhibit higher concentration and a downward shift in the mean. The main peak of the objective function becomes more prominent, the overall distribution range narrows, and the peak position shifts leftward compared to the unplanned case. This indicates that under the same level of source–load uncertainty, the total operating cost of the system decreases, and the optimal operating point becomes less sensitive to random disturbances. In addition, the dispersion among objective function samples is significantly reduced, showing that under complex conditions where wind and solar output fluctuations coexist with the spatiotemporal clustering of EV charging, the optimized system operation is more stable, presenting smaller cost fluctuations for the same uncertainty level. This demonstrates the enhanced robustness and cost predictability of the system after planning. Meanwhile, the probability of the distribution tail also contracts noticeably-particularly on the high-cost side-indicating that the cost impact of rare but extreme adverse scenarios

has been effectively mitigated. This finding aligns with the earlier conclusion from the voltage frequency distribution, where the "low-voltage tail shortening" phenomenon was observed: as voltage stability improves, line losses and voltage deviation penalties decrease correspondingly, achieving a synergistic improvement in both economic efficiency and operational security.

From a physical perspective, the convergence of the distribution is primarily driven by three synergistic mechanisms. First, the optimized selection of transformer capacity and substation location shortens power flow paths, leading to simultaneous reductions in both the mean value and fluctuation amplitude of the line loss term floss. Second, the coordinated control among reactive power regulation devices-such as capacitors and tap changers-effectively suppresses extreme scenarios in the voltage deviation term fv. Third, the optimized switching strategy enables smoother device operation, avoiding frequent large-scale actions and thereby reducing the probability of extreme values in the switching cost term fswitch. Collectively, these three mechanisms result in a global statistical trend characterized by an elevated main peak and a contracted tail in the frequency distribution of the objective function.

In summary, the frequency distribution results of the objective function fully demonstrate that the proposed distribution transformer layout planning method achieves comprehensive performance improvements in terms of lower average cost, reduced cost fluctuations, and mitigated tail risk in a probabilistic sense. Compared with traditional deterministic planning schemes based solely on typical operating conditions, this study incorporates joint modeling and scenario-based evaluation of wind-solar generation and EV charging behaviors. As a result, the optimization outcomes more accurately reflect the actual operational state distribution under high-penetration source-load conditions, thereby realizing enhanced economic efficiency and risk mitigation simultaneously at the planning level. This further verifies the engineering applicability and practical value of the proposed model in power systems with a high share of distributed generation and electric vehicles.

5 Conclusion

This study addresses the DT layout planning problem in distribution networks with high penetrations of DGs and EVs, and develops a multi-objective optimization model that explicitly incorporates source–load uncertainties. The stochastic characteristics of PV and wind power generation are represented using Beta and Weibull distributions, respectively, while the spatiotemporal

variability of EV charging demand is modeled through Monte Carlo simulation, thereby forming an integrated uncertainty characterization framework. DG output uncertainty primarily affects voltage rise and fluctuation during high-generation periods, while EV charging uncertainty mainly contributes to voltage drops and increased line loading during evening peaks.

Building on this foundation, an optimization planning scheme is constructed to minimize the total life-cycle cost-including transformer investment, network losses, and outage-related costs – while ensuring compliance with voltage, current, and equipment capacity constraints. Simulation studies based on an enhanced IEEE 33-bus system verify that the proposed model significantly improves voltage profile performance, reduces line losses, and lowers overall operational expenditure under complex multi-source and multi-load conditions. The improvement of voltage profiles and the reduction of power flow dispersion also help alleviate line loading stress and lower the risk of overload. Compared to traditional deterministic planning methods, the proposed framework shows clear advantages in transformer sizing rationality, voltage stability, and operational resilience.

In conclusion, the DT layout planning framework developed in this work provides both a systematic modeling methodology and a practical optimization strategy for distribution networks operating under high penetrations of DGs and EVs. It offers meaningful theoretical and engineering guidance for promoting low-carbon, intelligent, and resilient operation of modern distribution systems. Future research may further investigate the coordinated effects of energy storage systems and demand-response resources to develop more adaptive and cost-efficient integrated energy planning models.

Acknowledgment

This work is supported by the Science and Technology Project of Guangdong Power Grid Co., Ltd. (Contract No.: 0319002024030201DG00009).

References

[1] Misra A, Venkataramani G, Gowrishankar S, et al. Renewable energy based smart microgrids – A pathway to green port development[J]. Strategic Planning for Energy and the Environment, 2017, 37(2): 17–32.

[2] Verdejo, M. A., and Fernández, J. (2015). Prediction Model for the Electrical Industry in Spain – The Trend Toward Renewable Energy. Strategic Planning for Energy and the Environment, 35(3), 9–31.

[3] Luo, Y., Wang, W., Li, X., and Zhao, D. (2019). The Guangdong Emissions Trading Scheme. Strategic Planning for Energy and the Environment, 38(4), 42–62.

[4] X. Liu, C. Wang, X. Kong, Y. Zhang, W. Wang and K. Y. Lee, "Tube-Based Distributed MPC for Load Frequency Control of Power System With High Wind Power Penetration," in IEEE Transactions on Power Systems, vol. 39, no. 2, pp. 3118–3129, March 2024, doi: 10.1109/TPWRS.2023.3277997.

[5] X. Kong, X. Liu, L. Ma and K. Y. Lee, "Hierarchical Distributed Model Predictive Control of Standalone Wind/Solar/Battery Power System," in IEEE Transactions on Systems, Man, and Cybernetics: Systems, vol. 49, no. 8, pp. 1570–1581, Aug. 2019, doi: 10.1109/TSMC.2019.2897646.

[6] I. I. Ioannou, S. Javaid, C. Christophorou, V. Vassiliou, A. Pitsillides and Y. Tan, "A Distributed AI Framework for Nano-Grid Power Management and Control," in IEEE Access, vol. 12, pp. 43350–43377, 2024, doi: 10.1109/ACCESS.2024.3377926.

[7] Y. Liu, X. Lai, H. Xin, J. Zhu, L. Huang and S. Xia, "Generalized Short-Circuit Ratio Based Distributed Real-Time Stability Assessment of Renewable Power Systems," in IEEE Transactions on Power Systems, vol. 38, no. 6, pp. 5953–5956, Nov. 2023, doi: 10.1109/TPWRS.2023.3310795.

[8] J. Cheng, L. Wang and T. Pan, "Optimized Configuration of Distributed Power Generation Based on Multi-Stakeholder and Energy Storage Synergy," in IEEE Access, vol. 11, pp. 129773–129787, 2023, doi: 10.1109/ACCESS.2023.3334008.

[9] S. F. Abdelsamad, W. G. Morsi and T. S. Sidhu, "Impact of Wind-Based Distributed Generation on Electric Energy in Distribution Systems Embedded With Electric Vehicles," in IEEE Transactions on Sustainable Energy, vol. 6, no. 1, pp. 79–87, Jan. 2015, doi: 10.1109/TSTE.2014.2356551.

[10] B. R. Pereira, G. R. M. da Costa, J. Contreras and J. R. S. Mantovani, "Optimal Distributed Generation and Reactive Power Allocation in Electrical Distribution Systems," in IEEE Transactions on Sustainable Energy, vol. 7, no. 3, pp. 975–984, July 2016, doi: 10.1109/TSTE.2015.2512819.

[11] F. Yang, Q. Sun, Q. -L. Han and Z. Wu, "Cooperative Model Predictive Control for Distributed Photovoltaic Power Generation Systems," in IEEE Journal of Emerging and Selected Topics in Power Electronics,

vol. 4, no. 2, pp. 414–420, June 2016, doi: 10.1109/JESTPE.2016.2523546.

[12] E. C. da Silva, O. D. Melgar-Dominguez and R. Romero, "Simultaneous Distributed Generation and Electric Vehicles Hosting Capacity Assessment in Electric Distribution Systems," in IEEE Access, vol. 9, pp. 110927–110939, 2021, doi: 10.1109/ACCESS.2021.3102684.

[13] M. R. Islam, H. Lu, J. Hossain, M. R. Islam and L. Li, "Multiobjective Optimization Technique for Mitigating Unbalance and Improving Voltage Considering Higher Penetration of Electric Vehicles and Distributed Generation," in IEEE Systems Journal, vol. 14, no. 3, pp. 3676–3686, Sept. 2020, doi: 10.1109/JSYST.2020.2967752.

[14] R. Bayani, S. D. Manshadi, G. Liu, Y. Wang and R. Dai, "Autonomous Charging of Electric Vehicle Fleets to Enhance Renewable Generation Dispatchability," in CSEE Journal of Power and Energy Systems, vol. 8, no. 3, pp. 669–681, May 2022, doi: 10.17775/CSEEJPES.2020.04000.

[15] V. Murali and D. B. Raj, "Optimizing Electric Vehicle Charging Stations and Distributed Generators in Smart Grids: A Multi-Objective Meta-Heuristic Approach," in IEEE Latin America Transactions, vol. 23, no. 11, pp. 1022–1035, Nov. 2025, doi: 10.1109/TLA.2025.11194767.

[16] S. Dias Vasconcelos et al., "Assessment of Electric Vehicles Charging Grid Impact via Predictive Indicator," in IEEE Access, vol. 12, pp. 163307–163323, 2024, doi: 10.1109/ACCESS.2024.3482095.

[17] M. Abdelsattar, M. A. Ismeil, M. M. Aly and S. Saber Abu-Elwfa, "Analysis of Renewable Energy Sources and Electrical Vehicles Integration Into Microgrid," in IEEE Access, vol. 12, pp. 66822–66832, 2024, doi: 10.1109/ACCESS.2024.3399124.

[18] A. Demirci, S. M. Tercan, U. Cali and I. Nakir, "A Comprehensive Data Analysis of Electric Vehicle User Behaviors Toward Unlocking Vehicle-to-Grid Potential," in IEEE Access, vol. 11, pp. 9149–9165, 2023, doi: 10.1109/ACCESS.2023.3240102.

[19] E. C. da Silva, O. D. Melgar-Dominguez and R. Romero, "Simultaneous Distributed Generation and Electric Vehicles Hosting Capacity Assessment in Electric Distribution Systems," in IEEE Access, vol. 9, pp. 110927–110939, 2021, doi: 10.1109/ACCESS.2021.3102684.

[20] T. Zhang, Y. Huang, H. Liao, X. Gong and B. Peng, "Short-Term Power Forecasting and Uncertainty Analysis of Wind Farm at Multiple Time Scales," in IEEE Access, vol. 12, pp. 25129–25145, 2024, doi: 10.1109/ACCESS.2024.3365493.

[21] M. -U. -N. Khursheed et al., "PV Model Parameter Estimation Using Modified FPA With Dynamic Switch Probability and Step Size Function," in IEEE Access, vol. 9, pp. 42027–42044, 2021, doi: 10.1109/ACCESS.2021.3064757.

[22] C. He, J. Zhu, J. Lan, S. Li, W. Wu and H. Zhu, "Optimal Planning of Electric Vehicle Battery Centralized Charging Station Based on EV Load Forecasting," in IEEE Transactions on Industry Applications, vol. 58, no. 5, pp. 6557–6575, Sept.–Oct. 2022, doi: 10.1109/TIA.2022.3186870.

[23] N. Yaraghi, P. Tabesh, P. Guan and J. Zhuang, "Comparison of AHP and Monte Carlo AHP Under Different Levels of Uncertainty," in IEEE Transactions on Engineering Management, vol. 62, no. 1, pp. 122–132, Feb. 2015, doi: 10.1109/TEM.2014.2360082.

Biographies

Wenzhong Wang received the bachelor's degree from Tianhe College of Guangdong Polytechnic Normal University in 2010. He currently serves as a Planning Specialist in the Power Grid Planning Center of Dongguan Power Supply Bureau of Guangdong Power Grid Co., Ltd., with research focus on power grid planning.

Jinxing Zhong received the bachelor's degree from Guangdong Polytechnic Normal University in 2011 and a master's degree from Guangdong University of Technology in 2018. He currently serves as a Planning Specialist in the Power Grid Planning Center of Dongguan Power Supply Bureau of Guangdong Power Grid Co., Ltd., with research focuses including new-type power system planning and main power grid planning.

Jinping Zhang received the bachelor's degree from Tianjin University in 2013. She currently serves as a Researcher at the Intelligent Distribution Network Research Institute of Tianjin Tianda Qiushi Electric Power Technology Co., Ltd., with a research focus on power grid planning.

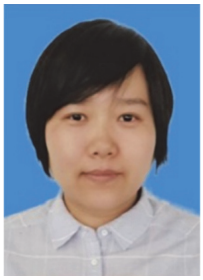

Juan Zhang received the bachelor's degree from Hebei University of Technology in 2012. She currently works as a Researcher at the Intelligent Distribution Network Research Institute of Tianjin Tianda Qiushi Electric Power Technology Co., Ltd., with a research focus on power grid planning.